JOURNAL OF CATALYSIS 154, 163–173 (1995)

Oxidative Coupling of Methane over Na_2WO_4/CeO_2 and Related Catalysts

Zhenqiang Yu, Xueming Yang, Jack H. Lunsford, and Michael P. Rosynek[1]

Department of Chemistry, Texas A & M University, College Station, Texas 77843

Received October 14, 1994; revised February 22, 1995

Na_2WO_4/CeO_2 is an active and selective catalyst for the oxidative coupling of methane (OCM). At 780°C and using a reactant feed of $CH_4:O_2:He = 4.8:1.0:5.6$, a C_2 selectivity in excess of 70% can be achieved over a 9.4 mol% Na_2WO_4/CeO_2 catalyst at a CH_4 conversion of 22%. By contrast, the C_2 selectivity exhibited by pure CeO_2 under the same reaction conditions, in the absence of Na_2WO_4 promoter, is <10%. The promoted catalyst is relatively insensitive to deactivation by formation of surface carbonate species. A comparable effect occurs for Na_2WO_4 on Pr_6O_{11}, which is also a nonselective catalyst in the absence of promoter. Characterization of Na_2WO_4/CeO_2 by X-ray powder diffraction, both after calcination and after use for the OCM reaction at 780°C, confirms that both the Na_2WO_4 and CeO_2 remain as discrete phases, and that no new bulk compounds or solid solutions are formed. X-ray photoelectron spectra demonstrate that all surface oxygen exists as lattice O^{2-} on the calcined catalysts and reveal no evidence for additional surface oxygen species, such as O_2^{2-} or O^-, that might serve as sites for CH_4 activation. Pulse reaction experiments show that bulk lattice oxygen species do not participate directly in the OCM reaction, and that the active oxygen species involved in the activation of methane exist only in the presence of gas phase oxygen. Ion scattering spectroscopy and *in situ* Raman spectroscopy indicate that the initial CeO_2 surface of the calcined catalyst is completely covered by one or more layers of Na_2WO_4, which exists in the molten state under reaction conditions.

INTRODUCTION

Lanthanide oxides have been extensively studied for the oxidative coupling of methane (OCM), and the basic sesquioxides, in both pure and promoted form, are among the most active and selective catalysts for this reaction (1). La_2O_3 itself, for example, is a reasonably effective OCM catalyst (2, 3); at 700–750°C and appropriate CH_4/O_2 reactant ratios, C_{2+} selectivities in excess of 60% can be achieved with unpromoted La_2O_3. Promotion with alkaline earth oxides, particularly those of Sr and Ba, improve the performance of La_2O_3 even further (4–7). Sm_2O_3 is a similarly effective OCM catalyst (8). The nature of the sites responsible for methane activation on these oxides remains uncertain. Otsuka concluded that peroxide (O_2^{2-}) sites were responsible for the activation of methane on Sm_2O_3 (8). Using an ESR technique, Wang and Lunsford (9) have demonstrated the existence of superoxide (O_2^-) ions on La_2O_3, whereas Dubois and Cameron (10) and Le Van *et al.* (3) found that $La_2O_2CO_3$ was stable at reaction temperature and was probably associated with methane activation.

Unlike the stoichiometric lanthanide sesquioxides, CeO_2 and PrO_x, which have multiple accessible cationic oxidation states, are highly active for methane conversion, but typically exhibit poor selectivity behaviors for the OCM reaction (10). The extremely high mobility of oxygen species in these materials results primarily in the formation of CO_x products during hydrocarbon oxidation reactions. The selectivity properties of these oxides can be markedly improved, however, by the addition of appropriate promoters. We have previously demonstrated, for example, that the addition of Na_2CO_3 transforms CeO_2 from a good methyl radical scavenger (and nonselective oxidation catalyst) into an effective material for the production of gas phase $CH_3\cdot$ radicals and, consequently, a selective methane coupling catalyst (11). $^3He^+$ ion scattering spectra (ISS) confirmed that the initial surface of the promoted CeO_2 was completely covered by Na_2CO_3, which was responsible for the high C_{2+} selectivity exhibited by this material.

Because of the significant promotional effect observed for Na_2CO_3/CeO_2, the present investigation was performed to determine the comparative promotional effects of other sodium salts on CeO_2 for the OCM reaction. In particular, Na_2WO_4 was selected for more extensive study because of its important role in a $Mn/Na_2WO_4/SiO_2$ catalyst that exhibits among the best overall activity/selectivity behaviors yet reported for OCM catalysts. A sustained C_{2+} selectivity of 65%, for example, has been observed at 37% CH_4 conversion (corresponding to a C_2 yield of 24%) over a 2 wt% Mn/5 wt% Na_2WO_4/SiO_2 catalyst at

[1] To whom correspondence should be addressed.

0021-9517/95 $6.00

800°C (12). We have confirmed this behavior in our own laboratory and have further demonstrated that a C_{2+} selectivity in excess of 80% can be sustained at 800°C over this catalyst at a CH_4 conversion of 20% (a 16% C_2 yield), in the absence of an inert diluent (13). A detailed understanding of the beneficial role played by Na_2WO_4 in this multicomponent catalyst has not yet been obtained. Jiang *et al.* (14) have recently suggested that the active species involves a surface cluster compound having the stoichiometry $Si_3WO_{8.5}$. However, virtually identical activity/selectivity behavior is observed over a $Mn/Na_2WO_4/MgO$ catalyst of comparable composition, indicating that the SiO_2 support is not an essential component (13).

EXPERIMENTAL

Materials

All reagents used for catalyst perparation were ACS certified grade. CeO_2 (99.9%) was obtained from Rhône-Poulenc, and the SiO_2 support was Grade 57 silica gel from Davison Chemical Co. All other chemicals were from Aldrich Chemical Co. Catalysts were prepared by dissolving the desired sodium salt in deionized water, adding an appropriate amount of the oxide support to the solution, and then evaporating the water until a thick paste was formed. The paste was dried at 120°C overnight and then calcined at 780°C in air for 6 h. Bulk compositions of selected Na_2WO_4/CeO_2 catalysts were determined by inductively coupled plasma (ICP) analysis, using a Perkin–Elmer Model 2000 ICP analyzer. Solutions were prepared for analysis by digesting a weighed catalyst sample for 1 h in concentrated nintric acid at 100°C and then adding one or two drops of 48 wt% HF solution. After removing the solution from the heat source, 1 to 2 ml of 50 wt% H_2O_2 were added to complete the dissolution of CeO_2 as the solution cooled to ambient temperature. The BET–N_2 surface areas and analyzed compositions of the SiO_2 and CeO_2 supports and of the series of supported Na_2WO_4 catalysts, which were the principal subject of this study, are summarized in Table 1. Prior to examining the catalytic behavior of the pure SiO_2 gel support in the absence of Na_2WO_4, it was first calcined in air for 6 h at 1000°C in order to decrease its surface area to a value comparable to those of the other catalysts studied.

Procedures

All catalytic experiments were performed using a downflow alumina reactor having an internal diameter of 10 mm. Quartz chips filled the space above the catalyst bed and served to preheat the reaction gases. An ice trap was used to remove the water in the product gases when a catalyst was kept on stream for several hours. Product gases were analyzed by gas chromatography, using a 13X molecular sieve column for separation of CH_4, O_2, and CO and a Haysept T packed column for separation of CH_4, CO_2, C_2H_4, C_2H_6, and higher hydrocarbons. Unless otherwise indicated, all experiments were performed at a reaction temperature of 780°C, using 1 g of catalyst and a feed mixture of $CH_4 : O_2 : He = 4.8 : 1.0 : 5.6$ at a total flow rate of 60 ml/mm and 1 atm total pressure. The carbon dioxide poisoning experiments were performed by including 5 to 30 Torr of added CO_2 to achieve the desired CO_2 partial pressure. The total flow rate in these cases was maintained at 100 ml/min by appropriate adjustment of the He diluent flow rate.

Pulse reaction experiments were performed using a microvolume system consisting of stainless steel valves and fittings and a 3.2-mm i.d. alumina reactor containing 0.2 g of catalyst. Pulses of CH_4 and/or O_2 were introduced by stainless steel switching valves into a 32 ml/min He carrier stream flowing over the catalyst sample. The resulting effluents were analyzed by gas chromatography.

Powder X-ray diffraction patterns of catalysts were obtained with a Rigaku RU-2000 automatic powder diffracto-

TABLE 1

Surface Areas of Catalysts and Supports

Material	SA (m^2/g)
SiO_2[a]	194
SiO_2[b]	2.4
CeO_2	7.5
Na_2WO_4	0.1
Na_2WO_4 (9.4 mol%) on:	
SiO_2	1.4
La_2O_3	1.8
Pr_6O_{11}	2.8
Nd_2O_3	2.9
Sm_2O_3	2.0
Dy_2O_3	3.4
Yb_2O_3	3.3

Na_2WO_4/CeO_2:

mol% Na_2WO_4		
Nominal	Analyzed (ICP)	SA (m^2/g)
1.0	1.3	5.1
2.6	2.6	4.3
5.2	5.3	3.7
7.8		2.8
9.4	9.7	2.4
11		2.1
13	13.1	2.0
21		1.5
30	27.8	1.3

[a] Used to prepare 9.4 mol% Na_2WO_4/SiO_2 catalyst.

[b] Used to obtain catalytic data in Table 2 for pure SiO_2 support.

meter equipped with a rotating anode generator operated at 50 kV and 180 mA. A Cu$K\alpha$ radiation source from a graphite monochromator was used in all cases. Patterns were obtained at 2°/min for the 2θ range 10°–70°.

XPS and ISS spectra were acquired using a Perkin–Elmer Model 5500 spectrometer equipped with an external stainless steel reaction system that allowed thermal and chemical pretreatments of samples at temperatures up to 600°C, followed by direct *in situ* introduction into the UHV analysis chamber. Samples requiring gas treatment and/or evacuation at temperatures >600°C were treated in a separate quartz reactor system that allowed *in situ* transfer of a ceramic holder containing the treated sample into an O-ring sealed stainless steel transport vessel that was subsequently attached to the XPS inlet system. Oxygen (99.99%), used for the *in situ* treatment of samples, was further purified by passage through a 13X molecular sieve column and a trap at 77 K. In a typical XPS data acquisition, a pass energy of 58.7 eV, a step increment of 0.125 eV, and a Mg anode power of 300 W provided an optimal combination of resolution and data collection time. All measured binding energies were referenced to the Au $4f_{7/2}$ peak at 83.8 eV resulting from sputter deposition of a small Au spot onto the sample. Near-surface compositions were calculated from peak areas in each spectral region, using appropriate sensitivity factors. ISS spectra were obtained using $^3He^+$ or $^{40}Ar^+$ ions at a scattering angle of 134.5° and 1 kV accelerating potential.

Raman spectra were obtained *in situ* for powdered samples using a Jobin Yvon Model U-1000 spectrometer equipped with a dual monochromator and both photomultiplier tube and charge-coupled device detectors. An argon ion laser line at 514.5 nm was used as the excitation light source. Prior to obtaining spectra, the pressed catalyst samples were pretreated in flowing O_2 at 800°C for 1 h, then cooled in flowing He to the desired temperature for data collection.

RESULTS AND DISCUSSION

Catalytic Experiments

The OCM behaviors of several Na_2WO_4-promoted lanthanide oxides and silica gel were initially surveyed by preparing catalysts containing 9.4 mol% of the promoter on each support. The resulting conversion/selectivity performances after 2 h of reaction at 780°C (to ensure steady-state behavior) are summarized in Table 2. For comparison purposes, the results for unpromoted La_2O_3, CeO_2, and Pr_6O_{11} are also shown, as well as data obtained with pure SiO_2 and Na_2WO_4/SiO_2, which were included in this study in order to establish the behavior of Na_2WO_4 on an essentially inert support that has virtually no activity for the selective activation of methane. Although the OCM selectivity behavior of SiO_2 is improved by the addition of Na_2WO_4, the supported catalyst continues to exhibit very low activity for methane conversion.

Under the reaction conditions employed for these experiments, the extent of CH_4 conversion was O_2-limited in most cases, except with the SiO_2 gel support; however, the comparative selectivity behaviors are significant. The promotional effect of Na_2WO_4 in enhancing C_2 selectivity was most pronounced for Pr_6O_{11} and particularly CeO_2, in agreement with reports by previous investigators under similar reaction conditions (15). The overall C_2 selectivity

TABLE 2

Activity/Selectivity Behaviors of Supported Na_2WO_4 Catalysts for Oxidative Coupling of Methane[a]

Support	CH_4 Conversion %	O_2 Conversion %	Selectivity (mol%) CO	CO_2	C_2H_4	C_2H_6	Total C_2's (%)	Specific rate [(mol/min/m^2) ($\times 10^5$)]
SiO_2[b]	1.1	7.6	42.4	15.1	9.3	11.8	21.1	
SiO_2	4.1	19.5	7.1	18.6	16.7	57.6	74.3	
La_2O_3[b]	23.4	96.5	5.6	42.8	26.4	25.2	51.6	
La_2O_3	25.8	97.0	2.6	44.1	28.7	24.6	53.3	14.
CeO_2[b]	14.2	93.4	9.7	84.0	2.8	3.5	6.3	
CeO_2	22.4	94.8	7.7	20.0	35.8	37.7	73.5	10.
Pr_6O_{11}[b]	21.2	93.2	11.2	79.6	4.1	5.1	9.2	
Pr_6O_{11}	27.6	94.5	0.1	37.5	29.5	32.8	62.3	9.7
Nd_2O_3	25.2	88.6	0.6	35.1	33.7	30.6	64.3	8.7
Sm_2O_3	26.3	92.5	1.0	35.6	33.1	30.2	63.4	13.
Tb_4O_7	26.6	95.4	0.1	43.7	25.1	31.0	56.1	
Dy_2O_3	22.7	88.1	2.8	38.7	28.4	30.0	58.4	6.7
Yb_2O_3	20.5	76.5	2.7	40.8	25.5	31.0	56.5	6.1

[a] T = 780°C; $CH_4 : O_2 : He$ = 4.8 : 1 : 5.6; total flow rate = 60 ml/min; 1 g catalyst; 9.4 mol% Na_2WO_4 on each support.
[b] Unpromoted oxide support.

of Na_2WO_4/CeO_2, in fact, was the highest exhibited by any of the catalysts examined under these conditions. By contrast, as shown by the results included in Table 2 for unpromoted La_2O_3, the C_2 selectivities of the Na_2WO_4-promoted Ln_2O_3 sesquioxides were not significantly different from the values (typically 50–60%) that have been observed previously for the unpromoted oxides (1). Although the substantial increase in both CH_4 conversion and C_2 selectivity over CeO_2 that is brought about by promotion with Na_2WO_4 could be attributed solely to the promoter, the very low CH_4 conversion observed in the case of Na_2WO_4/SiO_2 indicates that the CeO_2 may play an important role in activating O_2. The extent of O_2 conversion over Na_2WO_4/Yb_2O_3, for example, is considerably lower under these conditions than over Na_2WO_4/CeO_2.

Because of the marked improvement in selectivity brought about by the addition of Na_2WO_4 to CeO_2, the promotional effects of several other sodium salts were examined at similar loadings on this oxide. The results, again after 2 h of reaction in each case, are presented in Table 3. Although all of the sodium-containing promoters studied had a clearly beneficial effect on the normally poor C_2 selectivity of unpromoted CeO_2, the influences of NaCl and Na_2WO_4 were most pronounced. In the case of $NaCl/CeO_2$, however, both the activity and selectivity declined rapidly with increasing time on stream, whereas the behavior of Na_2WO_4/CeO_2 remained stable for much longer times of reaction. The CH_4 conversion of 27.8% and C_2 selectivity of 76.3% shown in Table 3 for $NaCl/CeO_2$ after 2 h of reaction, for example, decreased to only 8 and 40%, respectively, after 10 h on stream. By contrast, both the activity and the selectivity of the Na_2WO_4/CeO_2 catalyst after 10 h of reaction were virtually unchanged from the values shown in Table 3 for 2 h on stream.

In order to establish the loading level of promoter needed to attain the best overall activity/selectivity performance, a series of Na_2WO_4/CeO_2 catalysts containing various amounts of Na_2WO_4 was prepared and examined for OCM behavior at 780°C. As shown in Fig. 1, even relatively low loadings of the promoter caused a marked increase in C_2 selectivity, with the optimal CH_4 conversion and C_2 selectivity occurring in the range of 8 to 10 mol% Na_2WO_4. Consequently, all subsequent studies reported below were performed using a 9.4 mol% Na_2WO_4/CeO_2 catalyst.

The OCM behavior of this catalyst in the absence of an inert diluent ($CH_4:O_2 = 4.8$) was examined at various total reaction pressures in the range 1 to 5 atm. As shown in Table 4, both CH_4 conversion and total C_2 selectivity decreased slightly with increasing pressure. However, the C_2H_4/C_2H_6 ratio in the C_2 product was substantially enhanced at higher reaction pressures, increasing from a value of 1.0 at 1 atm to 2.4 at 5 atm.

OCM catalysts, particularly those containing alkali and/or alkaline earth oxides, often exhibit rapid and extensive deactivation due to surface carbonate formation by the CO_2 by-product of the coupling reaction (16). For this reason, the effect of added CO_2 on the activity/selectivity behavior of the 9.4 mol% Na_2WO_4/CeO_2 catalyst was investigated at 780°C and 1 atm pressure under nonoxygen-limiting reaction conditions (i.e., O_2 conversions of $\leq$70%). The CH_4 and O_2 partial pressures in these experiments were maintained at 320 and 67 Torr, respectively, with He and added CO_2 making up the balance to 760 Torr. Under these conditions, the partial pressure of CO_2 generated by the reaction itself was ~6 Torr, and, in the absence of added CO_2, the CH_4 conversion and C_2 selectivity were 11 and 76%, respectively. Addition of various CO_2 partial pressures to the feed stream had virtually no effect on either the activity or the selectivity of the catalyst. In the presence of a total CO_2 partial pressure as high as 47 Torr, for example, the CH_4 conversion and C_2 selectivity were still 10 and 72%, respectively. This

TABLE 3

Activity/Selectivity Behaviors of CeO_2-Supported Sodium Salts for Oxidative Coupling of Methane[a]

Sodium Salt	CH_4 Conversion (%)	O_2 Conversion (%)	Selectivity (mol%)				Total C_2's (%)
			CO	CO_2	C_2H_4	C_2H_6	
Na_2CO_3	19.4	81.0	8.6	38.9	20.5	32.0	52.5
Na_2WO_4	22.4	94.8	7.7	20.0	35.8	37.7	73.5
NaCl	27.8	93.2	12.3	11.4	58.0	18.3	76.3
Na_2SiO_3	20.7	92.6	12.6	24.6	28.1	34.7	62.8
Na_2SnO_3	21.6	94.0	18.2	16.8	29.0	36.1	65.1
Na_3PO_4	18.7	81.6	23.1	19.4	27.5	30.0	57.5
$Na_2B_4O_7$	19.1	83.0	18.6	28.4	21.6	31.4	53.0
Na_2SO_4	17.6	87.5	21.0	28.4	24.0	26.6	50.6

[a] T = 780°C; $CH_4:O_2:He$ = 4.8:1:5.6; total flow rate = 60 ml/min; 1 g catalyst; 9.4 mol% of sodium salt in each catalyst.

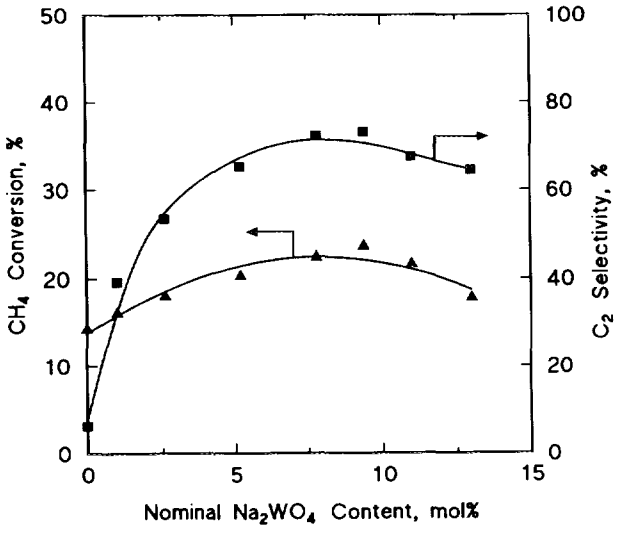

FIG. 1. Effect of Na_2WO_4 content on CH_4 conversion and C_2 selectivity over Na_2WO_4-promoted CeO_2 catalysts.

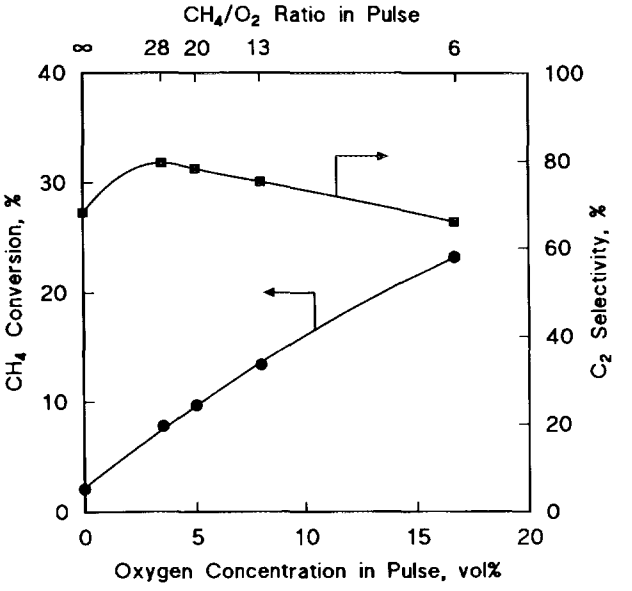

FIG. 2. Effect of CH_4/O_2 ratio on CH_4 conversion and C_2 selectivity in pulse reaction experiments over 9.4% Na_2WO_4/CeO_2 at 780°C (CH_4 concentration: 83.3 vol%, balance He).

lack of susceptibility to poisoning by CO_2 is evidently due to the inability of this catalyst to form a deactivating surface carbonate species at this temperature. Indeed, temperature-programmed desorption measurements revealed that no CO_2 remained on this catalyst at temperatures >400°C. The intentional addition of 5 mol% Na_2CO_3 to the 9.4 mol% Na_2WO_4/CeO_2 catalyst during its initial preparation, for example, caused its C_2 selectivity to decrease to that of the Na_2CO_3/CeO_2 catalyst shown in Table 3.

The possible participation of lattice oxygen species in either Na_2WO_4 or CeO_2 during the OCM process was explored by performing a series of experiments in which pulses containing varying CH_4/O_2 ratios were introduced into a He carrier passing over a 0.2-g sample of the 9.4 mol% Na_2WO_4/CeO_2 catalyst at 780°C. The CH_4 concentration in each pulse was maintained at 83.3 vol%, with the remainder consisting of He and O_2 in the proportions needed to achieve the desired CH_4/O_2 ratio, which was randomly varied. The CH_4 conversion for pulses containing no O_2 was only ~2%, as shown in Fig. 2. With increasing O_2 content in the pulse, however, the CH_4 conversion increased continuously, and at a CH_4/O_2 ratio of 6 (O_2 concentration = 16.7 vol%) the CH_4 conversion and C_2 selectivity approximated those observed in the flow experiments at a CH_4/O_2 ratio of 4.8 (Table 2). With the exception of the pulse containing no O_2, the C_2 selectivity decreased gradually with increasing O_2 concentration in the pulse.

Figure 3 presents additional information that was obtained from a second series of pulse reaction experiments, in which a pulse of pure O_2 was passed over the catalyst sample at 780°C, followed, at varying time intervals, by one of pure CH_4. (The time interval of zero between O_2 and CH_4 pulses corresponded to a single pulse, having a

TABLE 4

Effect of Reaction Pressure on Activity/Selectivity Behavior of 9.4 mol% Na_2WO_4/CeO_2 Catalyst for Oxidative Coupling of Methane[a]

Total pressure (atm)	CH_4 Conversion (%)	Selectivity (mol%)				
		CO	CO_2	C_2H_4	C_2H_6	Total C_2's (%)
1	22.1	7.7	20.0	36.8	37.7	74.5
2	21.5	2.5	27.5	41.5	30.0	71.5
3	19.5	2.1	29.8	42.1	26.0	68.1
4	19.2	1.8	33.7	43.4	21.2	64.5
5	19.0	1.7	36.0	44.2	18.1	62.3

[a] T = 782°C; $CH_4:O_2$ = 4.8:1, no He diluent; total flow rate = 60 ml/min; 1 g catalyst.

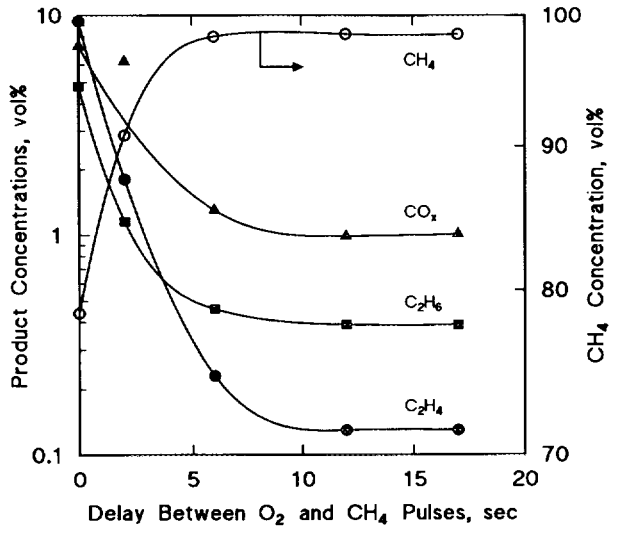

FIG. 3. Effect of delay time between O_2 and CH_4 pulses on amounts of products and unreacted CH_4 over 9.4% Na_2WO_4/CeO_2 catalyst at 780°C.

CH_4/O_2 ratio of 2/1.) As shown in Fig. 3, even a delay as short as 2 s between the O_2 and CH_4 pulses caused sharp decreases in the formation of both CO and C_2 products (note the logarithmic scale on the left-hand ordinate axis). For intervals of 6 s or longer between pulses, the extent of CH_4 conversion was negligible. Hence, we conclude from these results that catalyst bulk lattice oxygen species do not participate directly in the OCM reaction, and that the active oxygen species involved in the activation of methane exist only in the presence of gas phase oxygen. This conclusion is consistent with temperature-programmed desorption studies which indicated that all measurable adsorbed oxygen desorbs from this catalyst by ~250°C. A similar dependence on gaseous O_2 for sustaining the existence of the active surface oxygen species needed for CH_4 activation has been observed previously with a series of Ba/MgO catalyst, on which a surface peroxide entity requires the presence of a sufficiently high O_2 partial pressure for its occurrence (17, 18).

Catalyst Characterization

In order to obtain information about the principal components in these materials, X-ray powder diffraction (XRD) was used to identify bulk phases in the representative 9.4 mol% Na_2WO_4/CeO_2 catalyst. XRD analyses were based on the single most intense diffraction line of CeO_2, which occurs at a *d*-spacing of 3.138 Å, and on the three almost equally intense line of Na_2WO_4 at *d*-spacings of 5.330, 3.241, and 2.762 Å (19). The XRD patterns of the Na_2WO_4/CeO_2 catalyst, both after calcination and after use for the OCM reaction at 780°C, indicated the presence of only pure CeO_2 and Na_2WO_4 phases. Although diffraction lines for the latter phase were broadened slightly after catalytic use, no new bulk compounds or solid solution phases were observed. The absence of a measurable Na_2CO_3 phase is consistent with the above observation that the OCM activity of this catalyst is not poisoned by CO_2.

X-ray photoelectron and ion scattering spectroscopies were used to characterize the surface compositions of a series of freshly calcined Na_2WO_4/CeO_2 catalysts containing various Na_2WO_4 loadings, in an effort to obtain information about the nature of the surface sites that are responsible for CH_4 activation on these materials. The 9.4% Na_2WO_4/CeO_2 sample was also examined further after use as an OCM catalyst for 16 h at 780°C. Prior to XPS and ISS analyses, all samples were first pretreated in a flow of high-purity O_2 at 780°C for 6 h in a quartz reactor, cooled under O_2, and then transferred to the XPS sample introduction chamber without exposure to air.

XPS spectra in the O 1*s* region are presented in Fig. 4 for a series of Na_2WO_4/CeO_2 samples containing the indicated mol% of Na_2WO_4. Following the O_2 pretreatment described above, all samples displayed only a single O 1*s* peak, due to lattice O^{2-}, at a binding energy of ~530 eV. Both the location and shape of these peaks are indistinguishable from the O 1*s* spectra of pure CeO_2 and Na_2WO_4. (Because the melting point of Na_2WO_4 is ~700°C, the pure compound was pretreated in O_2 at only 500°C prior to XPS analysis.) Hence, additional near-surface oxygen-containing species, such as peroxide (O_2^{2-}), O^-, or OH, which typically exhibit O 1*s* binding energies 1 to 3 eV higher than O^{2-} (17) are not generated under these conditions. Furthermore, the C 1*s* spectra shown in Fig. 5 confirm the absence of a surface CO_3^{2-}

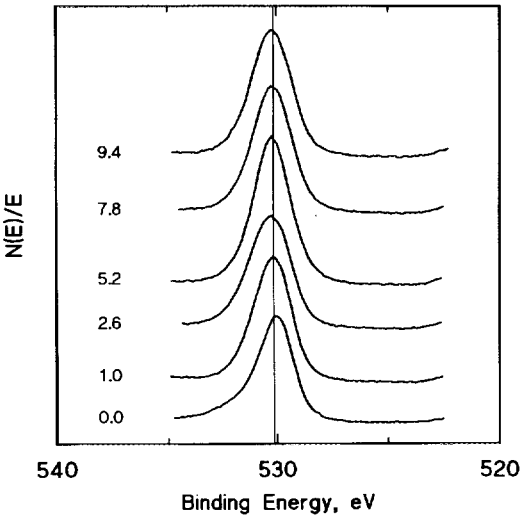

FIG. 4. XPS spectra in O 1*s* region for Na_2WO_4/CeO_2 catalysts containing the indicated mol% loading of Na_2WO_4 after exposure to oxygen at 600°C for 15 min, followed by evacuation at 600°C.

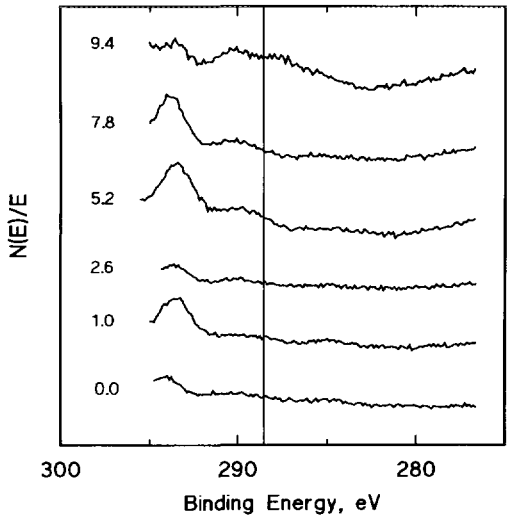

FIG. 5. XPS spectra in C 1*s* region for Na_2WO_4/CeO_2 catalysts containing the indicated mol% loading of Na_2WO_4 after exposure to oxygen at 600°C for 15 min, followed by evacuation at 600°C.

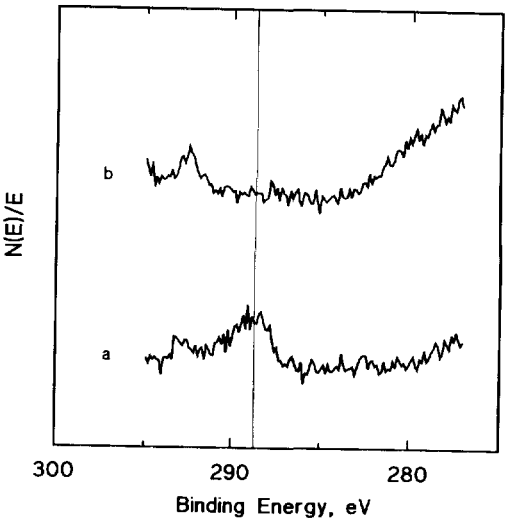

FIG. 7. XPS spectra in C 1*s* region for 9.4 mol% Na_2WO_4 on (a) La_2O_3 and (b) Pr_6O_{11}.

species, which would produce a C 1*s* peak at ~288 eV. By way of contrast, corresponding XPS spectra for 9.4 mol% Na_2WO_4 on La_2O_3 and Pr_6O_{11} supports are shown in Figs. 6 and 7. In spectrum a in Fig. 6, the peak centered at ~529 eV contains contributions from lattice O^{2-} species in both La_2O_3 and Na_2WO_4, while the peak at ~532 eV is due to the oxygen in surface CO_3^{2-} (and possibly OH) species, as shown by the C 1*s* peak at ~288 eV in spectrum a of Fig. 7. The O 1*s* spectrum (Fig. 6b) is virtually identical to that of pure Pr_6O_{11}, in which Pr occurs in both the +3 and +4 oxidation states, giving rise to differing chemical environments for the lattice O^{2-} species and the observed two-peak spectrum. The O^{2-} contribution from Na_2WO_4 is contained within the overall O 1*s* envelope

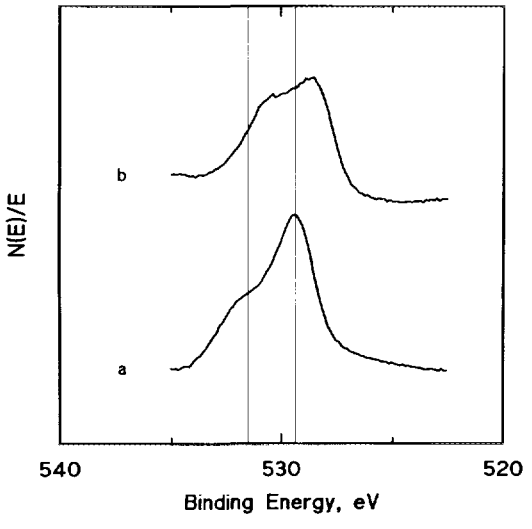

FIG. 6. XPS spectra in O 1*s* region for 9.4 mol% Na_2WO_4 on (a) La_2O_3 and (b) Pr_6O_{11}.

and cannot be separately distinguished. Unlike the case with La_2O_3, no measurable surface CO_3^{2-} occurred with the Pr_6O_{11} support, as confirmed by the absence of a peak at ~288 eV in the C 1*s* spectrum of this catalyst (spectrum b in Fig. 7).

The near-surface compositions of the catalysts studied, based on corrected XPS peak areas in the C 1*s*, O 1*s*, Na 1*s*, Ce 3*d*, and W 4*f* regions, are summarized in Table 5. The W/Ce surface ratio increased with increasing Na_2WO_4 loading up to 4.2 mol%, but then remained relatively constant with further increase in Na_2WO_4 content. These changes in the W/Ce ratio closely parallel those in the corresponding C_2 selectivities exhibited by these catalysts for the OCM reaction (Fig. 1). These results are also consistent with calculations (based on the unit cell size of Na_2WO_4 and the surface area of the CeO_2 support) which indicate that uniform monolayer coverage of Na_2WO_4 on CeO_2 would occur at a Na_2WO_4 loading of ca. 5 mol%. Although such homogeneous coverage would be unusual for most supported oxide catalyst systems, it is not unreasonable in the present case because the 780°C temperature employed for both pretreatment and catalytic reaction studies considerably exceeds the melting point (~700°C) of Na_2WO_4, thus promoting its uniform distribution across the CeO_2 surface. Recrystallization of the molten Na_2WO_4 phase upon cooling may produce sufficiently large crystals of the solidified salt that the observed W/Ce surface ratio remains essentially constant at all Na_2WO_4 contents larger than that required for such crystallite formation.

The effect of such thermal treatment on the phase behavior and possible fusion of Na_2WO_4 on CeO_2 was investigated further by *in situ* Raman spectroscopy. Crystalline Na_2WO_4 exists in a spinel structure having tetrahedral site

TABLE 5

Surface Compositions of Na_2WO_4/CeO_2 Catalysts

Na_2WO_4 (mol %)	Surface Composition (at.%)						
	C 1*s*	O 1*s*	Ce 3*d*	Na 1*s*	W 4*f*	W/Ce	Na/Ce
0	0	68	32				
1	0.2	69	24	0.7	5.8	0.24	0.03
2.6	0.2	65	18	4.2	8.9	0.5	0.24
4.2	0.2	69	12	5.6	13	1.0	0.46
6.2	0.8	64	12	9.7	14	1.2	0.84
8.1	0.9	65	10	13	11	1.1	1.2
9.4	0.6	63	11	15	11	1.0	1.4

symmetry. Its Raman spectrum at ambient temperature exhibits four fundamental vibrational modes at 928 cm^{-1} (A_1), 312 cm^{-1} (E), 813 cm^{-1} (F_2), and 373 cm^{-1} (F_2), as well as a lattice vibration at 93 cm^{-1} that is characteristic of the crystalline state (20). The *in situ* Raman spectra shown in Figs. 8 and 9 were obtained in random order for a sample of the 30 mol% Na_2WO_4/CeO_2 catalyst that was maintained at each of the indicated temperatures. The intense band that appears at 450 cm^{-1} in all of the spectra in Fig. 8 is due to CeO_2. The bands at 304, 804, and 921 cm^{-1} in the spectrum at 500°C correspond to the E, F_2, and A_1 fundamental vibrational modes of Na_2WO_4, and have all been shifted slightly to lower frequencies due to thermal expansion of the crystal lattice. (The additional F_2 fundamental mode that occurs at 373 cm^{-1} in the ambient spectrum of Na_2WO_4 is very weak and does not appear in Fig. 8.) The lattice vibration characteristic of the crystalline state is also slightly red-shifted due to thermal effects, and appears at 86 cm^{-1} in Fig. 9.

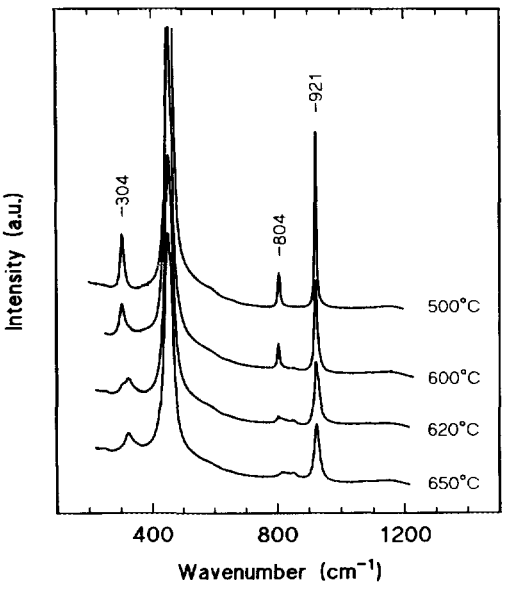

FIG. 8. Raman spectra in the region 200–1200 cm^{-1} of 30 mol% Na_2WO_4/CeO_2 in He at 500–650°C.

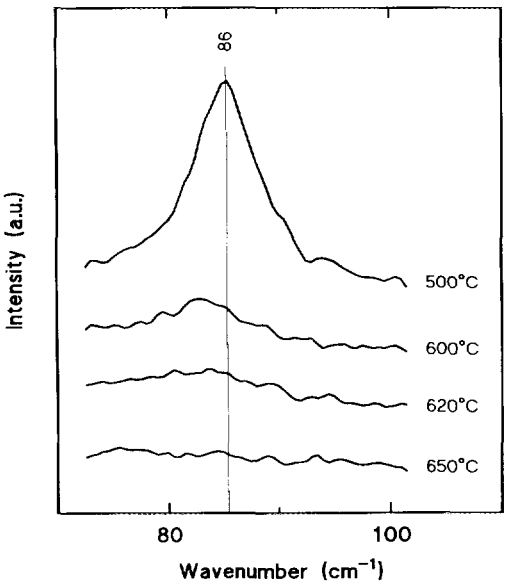

FIG. 9. Raman spectra in the region 70–110 cm^{-1} of 30 mol% Na_2WO_4/CeO_2 in He at 500–650°C.

With increasing sample temperature, the latter band decreases significantly in intensity and disappears completely at 620–650°C, indicting that the previously crystalline material had melted. By contrast, the other bands due to Na_2WO_4 at higher frequencies do not disappear at this temperature, although their intensities are attenuated and the structures of certain of them, particularly those at 304 and 804 cm^{-1}, become modified. Additional weak bands also appear in these spectral regions with increasing temperature, due to distortion of the ideal tetrahedral structure and resulting decreased symmetry that make additional vibrational modes become Raman active (20). The characteristic lattice vibration band at 86 cm^{-1} reappears when the temperature is decreased to below ~650°C, indicating that the process is reversible and that Na_2WO_4 recrystallizes on the CeO_2 support. The bands at 304, 804, and 921 cm^{-1} also return to their original intensities and frequencies upon cooling. These results confirm that not only does Na_2WO_4 undergo melting and recrystallization on the CeO_2 support during thermal pretreatment, but that fusion occurs at an even lower temperature than the normal melting point of the crystalline salt, viz., 698°C. Hence, it is likely that the active Na_2WO_4 component exists in the liquid phase at the OCM reaction temperature of 780°C employed in the present investigation.

In contrast to the virtually constant near-surface W/Ce ratio exhibited at Na_2WO_4 loadings ≥4.2 mol% (Table 5), the corresponding Na/Ce surface ratio increases continuously with increasing Na_2WO_4 loading. Additionally, the

Na/W ratio for all of the catalysts is substantially lower than the expected stoichiometric value of 2/1, particularly at low Na_2WO_4 loadings. This behavior suggests that Na may migrate into the CeO_2 lattice, perhaps as a Na_xO phase, thus causing the Na_2WO_4 loading needed for optimal OCM activity/selectivity (8–10 mol%, Fig. 1) to exceed the monolayer value of ca. 5 mol%. Such lattice penetration by Na could result in an XPS-detectable near-surface region that contains, for example, a $Ce(WO_4)_x$ phase, in addition to CeO_2 and remaining Na_2WO_4, hence producing the low Na/Ce and Na/W ratios that are observed. The existence of a near-surface Na_2O species would, in any case, not be detected by XPS, since the O 1*s* binding energy of this compound is virtually identical to that of CeO_2 and Na_2WO_4.

In a previous investigation, XPS spectra of a 10.7 mol% Na_2CO_3/CeO_2 catalyst that had been used for the OCM reaction at 775°C exhibited a Na/Ce ratio of 3.7, indicating that the near-surface region of the catalyst had become enriched in Na, since the bulk Na/Ce ratio of this material was only 0.24 (11). Furthermore, ^{3}He ISS spectra of the used catalyst contained no peak due to Ce, indicating that the CeO_2 surface was completely covered by Na_2CO_3. ^{3}He ISS spectra are presented in Fig. 10 for the O_2-treated 9.4 mol% Na_2WO_4/CeO_2 catalyst and, for comparison purposes, for pure CeO_2 and Na_2WO_4. It is apparent that the spectrum of the Na_2WO_4/CeO_2 catalyst, although containing more than 90 mol% CeO_2, closely resembles that of pure Na_2WO_4. However, it is not possible to unambiguously conclude from these results that the CeO_2 surface is completely covered by Na_2WO_4 because scattered ^{3}He ions provide insufficient resolution at high $E/E(0)$ ratios to give separate peaks for Ce and W. For this reason, additional ISS data were obtained using an ^{40}Ar ion source.

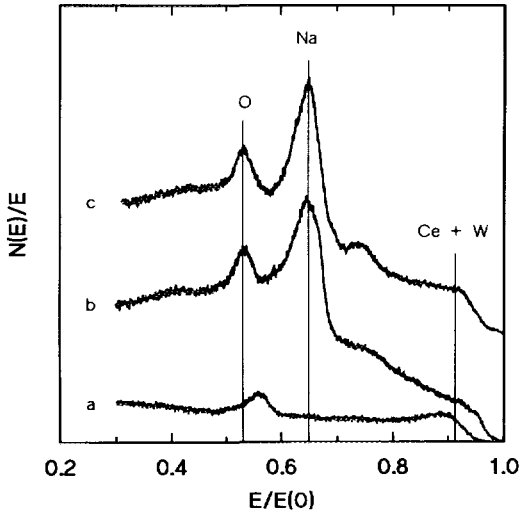

FIG. 10. ^{3}He ISS spectra of: (a) CeO_2; (b) 9.4% Na_2WO_4/CeO_2; and (c) Na_2WO_4 after treatment in O_2 at 780°C for 4 h, followed by evacuation at 780°C.

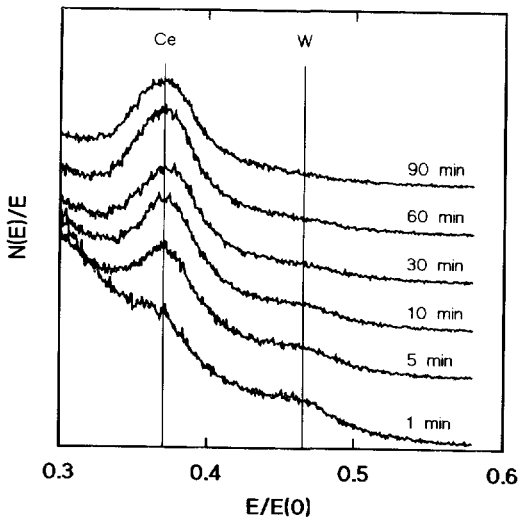

FIG. 11. ^{40}Ar ISS spectra of 9.4% Na_2WO_4/CeO_2 for various sputtering times.

The extent of sputtering and consequent surface modification during ISS data collection is much greater when using ^{40}Ar ions than that which occurs with ^{3}He ions, even at the incident ion energy of ~1 keV used in these experiments. Figure 11, for example, presents ^{40}Ar ISS spectra that were recorded after various data collection times for the O_2-treated 9.4% Na_2WO_4/CeO_2 catalyst. The resulting Ce and W peak areas are plotted as a function of total sputtering time in Fig. 12. Although the Ce and W scattering peaks are well resolved using ^{40}Ar ions, it is apparent that the composition of the uppermost surface layer changes rapidly during exposure to the ion source,

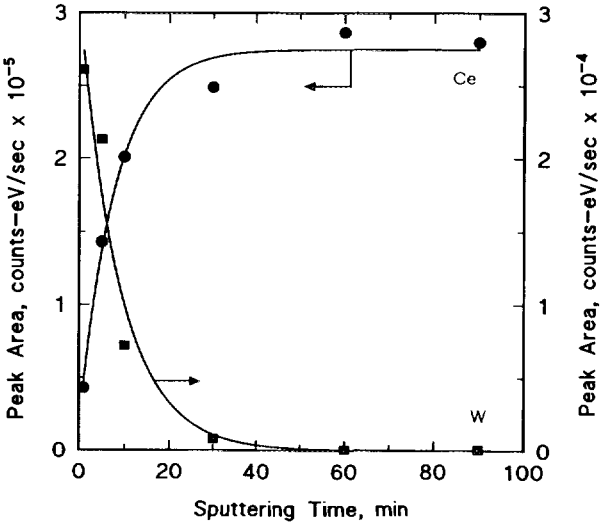

FIG. 12. Effect of sputtering time on ^{40}Ar ISS peak areas of Ce and W for 9.4% Na_2WO_4/CeO_2.

an effect that was not observed with the ^3He ISS spectra. Extrapolation of the Ce and W peak areas to zero sputtering time, however, confirms that the CeO_2 surface in the catalyst was initially covered completely by a Na_2WO_4 phase. This coverage behavior is similar to that observed previously for Na_2CO_3/CeO_2 (11).

In order to further characterize the surface compositions of a series of Na_2WO_4/CeO_2 catalysts containing varying loadings of Na_2WO_4, the additional ^{40}Ar ISS spectra shown in Fig. 13 were each obtained after 1 min of exposure to the ion source. The resulting W/Ce peak area ratios are shown in Fig. 14. The W/Ce surface ratio increases continuously with increasing Na_2WO_4 content, and in the 30 mol% Na_2WO_4/CeO_2 sample (not shown in Fig. 14), Ce is not detectable in the surface layer, even after 1 min of sputtering. Extrapolation to zero ion exposure of the W/Ce ratios obtained for each catalyst at various sputtering times indicated that the CeO_2 in all samples containing ≥5.3 mol% of Na_2WO_4 was completely covered by the promoter.

CONCLUSION

The addition of Na_2WO_4 to CeO_2 or Pr_6O_{11} transforms these oxides from nonselective, total oxidation catalysts into reasonably active and selective catalysts for the oxidative coupling of methane. Na_2WO_4 remains as a discrete phase on CeO_2, even after calcination and use as an OCM catalyst at 780°C, and no new bulk compounds or solid solutions detectable by XRD are formed under these conditions. Surface carbonate species do not readily form on these materials, making them relatively insensitive to deactivation by the CO_2 by-product of the OCM reaction. The nature of the sites responsible for CH_4 activation

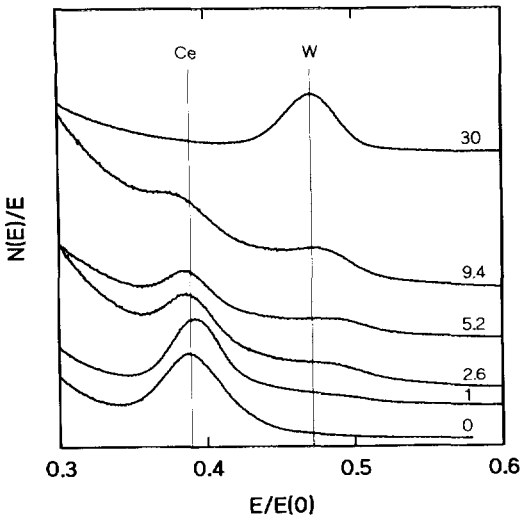

FIG. 13. ^{40}Ar ISS spectra for Na_2WO_4/CeO_2 catalysts containing the indicated mol% loading of Na_2WO_4.

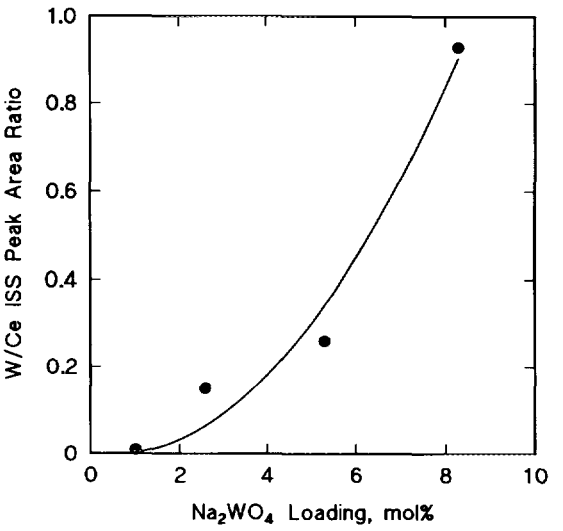

FIG. 14. Effect of Na_2WO_4 content on surface W/Ce ratio from ^{40}Ar ISS spectra for Na_2WO_4/CeO_2 catalysts.

remains unclear, but it is certain that bulk lattice O^{2-} species are not directly involved, since the existence of the active sites is sustained only in the presence of gaseous O_2. No evidence for surface oxygen species such as O^- or O_2^{2-} was observed. At OCM reaction temperatures ≥ ~700°C, and at Na_2WO_4 loadings > ~4 mol%, the CeO_2 surface of the calcined catalyst is completely covered by molten Na_2WO_4. However, as shown by comparison with the behavior of Na_2WO_4/SiO_2 (Table 2), the CeO_2 still plays an important role in the activations of CH_4 and O_2. Cerium ions from the support may, for example, become dispersed in the molten phase and react with gaseous O_2 to produce an active form of oxygen which, in turn, generates $CH_3\cdot$ radicals by abstracting H atoms from CH_4 molecules. Thus, the overall catalytic reaction may occur in a three-phase system in which the nonselective CeO_2 phase is passivated by Na_2WO_4. Similar phenomena may be responsible for the favorable OCM results obtained with the Na_2WO_4/Pr_6O_{11} catalyst.

ACKNOWLEDGMENT

The authors gratefully acknowledge financial support of this research by the National Science Foundation under Grant CHE-9005808.

REFERENCES

1. Lunsford, J. H., *in* "New Frontiers in Catalysis" (L. Guczi *et al.*, Eds.), Elsevier, Amsterdam, 1993.
2. Sugiyama, S., Matsumura, Y., and Moffat, J. B., *J. Catal.* **139,** 338 (1993).
3. LeVan, T., Che, M., Tatibouët, J. M., and Kermarec, M., *J. Catal.* **142,** 18 (1993).
4. Ilett, D. J., and Islam, M. S., *J. Chem. Soc. Farad. Trans.* **89,** 3833 (1993).
5. Yamashita, H., Machida, Y., and Tomita, A., *Appl. Catal. A: General* **79,** 203 (1991).

6. Mimoun, H., Robine, A., Bonnaudet, S., and Cameron, C. J., *Chem. Lett.*, 2185 (1989).
7. Lin, C. H., Campbell, K. D., Wang, J. X., and Lunsford, J. H., *J. Phys. Chem.* **90,** 534 (1986).
8. Otsuka, K., Said, A. A., Jinno, K., and Komatsu, T., *Chem. Lett.*, 77 (1987).
9. Wang, J. X., and Lunsford, J. H., *J. Phys. Chem.* **90,** 3890 (1986).
10. Dubois, J. L., and Cameron, C. J., *Appl. Catal.* **67,** 49 (1990).
11. Tong, Y., Rosynek, M. P., and Lunsford, J. H., *J. Catal.* **126,** 291 (1990).
12. Fang, X., Li, S., Lin, J., Gu, J., and Yan, D., *J. Mol. Catal. (China)* **6,** 255 (1992).
13. Wang, D., Rosynek, M. P., and Lunsford, J. H., unpublished results.
14. Jiang, Z. C., Yu, C. J., Fang, X. P., Li, S. B., and Wang, H. L., *J. Phys. Chem.* **97,** 12,870 (1993).
15. DeBoy, J. M., and Hicks, R. F., *Ind. Eng. Chem. Res.* **27,** 1577 (1988).
16. Lunsford, J. H., Hinson, P. G., Rosynek, M. P., Shi, C., Xu, M., and Yang, X., *J. Catal.* **147,** 301 (1994).
17. Dissanayake, D., Lunsford, J. H., and Rosynek, M. P., *J. Catal.* **143,** 286 (1993).
18. Rosynek, M. P., Dissanayake, D., and Lunsford, J. H., *in* "New Developments in Selective Oxidation II" (V. C. Corberán and S. V. Bellón, Eds.), Elsevier, Amsterdam, 1994.
19. Powder Diffraction File, JCPDS International Centre for Diffraction Data, 1980.
20. Horsley, J. A., Wachs, I. E., Brown, J. M., Via, G. H., and Hardcastle, F. D., *J. Phys. Chem.* **91,** 4014 (1987).